energy&fuels

Environmental and Carbon Dioxide Issues

Adsorption of crude oil components at mineral surfaces followed by quartz crystal micro-balance and contact angle measurements: The effect of oil composition, simulated weathering and dispersants

Umer Farooq, Meysam Nourani, Flavien Ivol, Anne Bjerke Årrestad, and Gisle Øye

Energy Fuels, **Just Accepted Manuscript** • DOI: 10.1021/acs.energyfuels.8b03084 • Publication Date (Web): 01 Mar 2019

ACS Publications

is published by the American Chemical Society. 1155 Sixteenth Street N.W., Washington, DC 20036

Adsorption of Crude Oil Components at Mineral Surfaces followed by Quartz Crystal Microbalance and Contact Angle Measurements: The Effect of Oil Composition, Simulated Weathering and Dispersants

Umer Farooq[†,*], Meysam Nourani‡, Flavien Ivol[‡], Anne Bjerke Årrestad[‡] and Gisle Øye[‡,*]

[†] SINTEF Ocean, Department of Environment and New Resources, Trondheim-Norway
[‡] Ugelstad Laboratory, Department of Chemical Engineering, Norwegian University of Science and Technology (NTNU), Trondheim, Norway
*Corresponding authors: gisle.oye@chemeng.ntnu.no; umer.farooq@sintef.no

ABSTRACT:

Improved knowledge of interactions between crude oil and solid surfaces is of great importance for understanding oil spill responses as well as oil spill behaviour on land and in the near shore environment. Here, the goal was to study how crude oils with various physicochemical properties interacted with model shoreline surfaces. In addition, the influence of simulated weathering and addition of dispersant was investigated for selected crude oils. A quartz crystal microbalance was used to follow the adsorption from 13 different crude oils on silica, aluminosilicate and calcium carbonated surfaces, while the corresponding wettability alterations were followed by contact angle measurements. The polar crude oil components adsorbed in considerably higher amounts on the calcium carbonate surfaces than on the silica and aluminosilicate surfaces. The simulated weathering of oils resulted in increased adsorption onto both the silica and aluminosilicate surface, while it had little effect on the calcium carbonate surface. The presence of dispersants generally reduced the amounts adsorbed on the surfaces. In the presence of seawater, the crude oil with higher total acid number interacted strongest with the calcium carbonate surface.

Key words: Oil spills, Shoreline surfaces, Quartz crystal microbalance, Wettability, Adsorption, Crude oil components

1. INTRODUCTION

Marine oil spills have become more frequent over the last few decades as offshore oil production and transport have increased [1, 2]. In 2010, the world experienced the largest offshore oil spill in history when BP's Deepwater Horizon had a blowout causing more than 4 million barrels of crude oil entering the Gulf of Mexico [3, 4]. Oil tankers carrying millions of gallons of oil can also pose a significant threat to the marine environment in the event of collisions or grounding [5]. If oil is spilled at sea, the objective of the response is to prevent the oil from reaching the shoreline. This is mainly due to more difficult cleanup processes of shorelines compared to cleanup and containment at sea [6]. If the oil becomes deposited or stranded on the shoreline, however, the choice of cleanup process should as far as possible be based on the behavior of the oil. Multiple factors can influence this behavior, including the physicochemical properties of the crude oil, the type of shoreline, water salinity and turbulence in the sea. Furthermore, the properties of crude oils might change after spillage due to physical and biological processes, referred to as weathering [7]. Fresh oils have been found to be less adhesive to shorelines than weathered oils, while light oils are considered less adhesive than heavier oils [8, 9].

The application of oil spill dispersants is an important part of the "toolbox" for responding to oil spills. Typically, the dispersants are sprayed on oil slicks at the surface, to break the oil into small droplets and accelerate the dispersion into the water column [10]. In this way the oil becomes removed from the surface of the sea and is more available for biodegradation by naturally occurring microorganisms [11]. Parameters affecting the performance of dispersants include their amount, mixing energy, crude oil properties, temperature and salinity of the water. Furthermore, changes in physical and chemical properties of the oil will influence how well dispersants interact with the oil. One example is decreased efficiency of dispersants for highly viscous oils, explained

by inhibited transport of surfactants to the oil-water interface and thereby increased energy requirements to break up droplets from the oil slick [12].

Crude oils are complex mixtures of saturated, unsaturated and aromatic compounds that contain various fractions of metals and heteroatoms such as nitrogen, sulphur and oxygen [13, 14]. The detailed composition depends on the geological formation where the oil is found and varies from field to field and even from well to well [8]. The unique physiochemical properties for each oil make it crucial to understand how they will behave on the surface of the sea and interact with shorelines to evaluate possible oil spill responses and the effects on the environment [15].

Understanding of the interactions between crude oil components and mineral surfaces can be a useful way to improve knowledge of the shoreline behavior of oils [16, 17]. Such interactions can generally occur through four mechanisms [18, 19]: (1) Polar interactions resulting in adsorption in the absence of water. (2) Surface precipitation if the oil becomes a poor solvent for its asphaltenes. (3) Acid/base interactions in the presence of water. (4) Ion-binding interactions, where multivalent cations will bind charged compounds present at the oil/water interface to oppositely charged sites at the mineral surfaces. All these mechanisms can lead to wettability alterations. Several authors have reported that small amounts of asphaltenes and resins in the crude oil can make originally water-wet surfaces more oil wet [20, 21]. The importance of asphaltenes was emphasized by observations that de-asphalted crude oil did not exhibit adhesion[18]. Acidic and basic components of crude oil have also been found important for wettability alterations [22-24]. Furthermore, the quartz crystal microbalance (QCM) technique has been introduced as a useful method of studying adsorption of crude oil components on various surfaces [25-29].

Contact angle measurements are widely used to evaluate wetting properties of liquids on solid surfaces. When a drop of liquid is deposited on the solid surface, an angle θ is formed. If this angle is less than 90^{o}, the liquid is wetting the surface. This method has been applied to study the interactions between oil and various surfaces [30-33].

The purpose of this work was to investigate how model shoreline surfaces interacted with crude oils with different physicochemical properties. Silica, aluminosilicate and calcium carbonate were chosen as model surfaces to represent abundant shoreline minerals. A quartz crystal microbalance with dissipation monitoring (QCM-D) was used to follow the adsorption of components from 13 crude oils onto these surfaces, while the corresponding wettability alterations were followed by contact angle measurements. The influence of simulated weathering (i.e. evaporation loss of light hydrocarbon components by distillation) and addition of dispersant on selected crude oils was also investigated.

2. MATERIALS AND METHODS

2.1. Crude Oils

Crude oils were selected based on their different physical and chemical properties. Generally, crude oils are divided into four main categories i.e. asphaltic, naphthenic, paraffinic and waxy crude oils. Thirteen crude oils denoted A-M were selected from all four categories and were further investigated. The total acid number (TAN), total base number (TBN), asphaltene content, wax content, density and viscosity of the oils were determined according to standard procedures [34-39].

The physicochemical properties of the investigated crude oils are listed in Table 1. The total acid number (TAN) was low for most oils, ranging from 0.1 to 0.4 mg/g. Only crude oil A and crude oils G had significantly higher acid content of 2.1 and 1.1 mg/g, respectively. Overall, the total base numbers (TBN) were higher than the acid numbers. When detectable, TBN varied between 1.0 and 3.2 mg/g for most oils, while crude oil D had a significantly higher base content (7.1 mg/g). This oil also had the highest asphaltene content (6.6 wt%), while it was lower than 1.8 wt% for the other oils. The wax content varied from 1.1 to 4.6 wt%. Both viscosity and density were considerably higher for crude oil A (708 mPas and 0.94 g/ml) and crude oil D (867 mPas and 0.93 g/ml). The remaining densities and viscosities of the oils were lower than 0.90 g/ml and 64 mPas, respectively.

2.2. Evaporation of Crude Oils

Four crude oils (A, F, H and L) were treated to simulate the evaporation loss of lighter crude oil components during 0.5-1 day of weathering on the sea surface. The evaporation was carried out

as a simple one-step distillation at vapour temperatures of 200°C [40]. The residues were referred to as weathered fractions and the physicochemical properties were determined as above.

2.3. Addition of Dispersant

A dispersant (Corexit® 9500A) was mixed with the selected crude oils and weathered fractions in dispersant to oil weight ratio (DOR) of 1:100. Corexit® 9500A (NALCO Environmental Solutions LLC, USA) contains a mixture of nonionic (48%) and anionic (35%) surfactants and at breaking wave sea conditions, DOR of 1:100 or less can be adequate for effective dispersion [8].

2.4. Quartz Crystal Microbalance (QCM) Measurements

Principle:

The dissipative quartz crystal microbalance (QCM-D) measures simultaneously changes in resonance frequency and dissipation of an oscillating quartz crystal. The quartz crystal is sandwiched between two electrodes, where one is coated with a thin surface film. Upon application of AC voltage, the crystal vibrates with a characteristic frequency which changes when the oscillating crystal is brought in contact with solutions. This change in frequency can be related to the following factors: (1) mass loading (2) liquid loading and (3) liquid trapping. The mass of the adhering layer can be determined by the Sauerbrey equation:

$$\Delta f_{ads} = -\frac{2nf_0^2\Delta m}{\rho_q v_q A} = -\frac{n\Delta m}{C} \qquad (1)$$

where f_o is the fundamental resonance frequency (5×10^6 Hz), n is the number of overtone, Δm is the adsorbed mass, A is the active area of the crystal (0.785 cm^2), ρ_q is the specific density of quartz (2650 kg/m^3), v_q is the shear wave velocity in quartz (3340 m/s), and C is a characteristic quartz crystal constant (17.7 ng Hz^{-1} cm^{-2} for a 5 MHz crystal).

Procedures:

A QCM-Z500 (KSV, Helsinki, Finland) was used to study the adsorption of crude oil components onto quartz crystal surfaces coated with silica, aluminosilicate and calcium carbonate. The adsorption was carried out from solutions where crude oils and weathered fractions (with and without dispersant) were diluted to 10 wt% in toluene (VWR, 99.5 %). To ensure homogenous mixing and dissolution, the solutions were placed on a vibrator for 1 hour, and then stored in a dark, cold placed for future use. The dilution of the crude oils eliminated any density and viscosity effects and emphasized the variation of the chemical components during the adsorption experiments.

Prior to each measurement contamination was removed from the crystal surfaces by rinsing with excess toluene (VWR, 98%) followed by ion-exchanged water (MQ water, Ω = 18.2 MΩ.cm, Millipore Simplicity System). Then the crystals were blow-dried with air and placed in an aqueous 2wt % sodium dodecyl sulfate solution for 30 minutes. For the calcium carbonate crystals, the sodium dodecyl sulfate solution was replaced by toluene. All the crystals were then rinsed with MQ water and dried with air. The dry crystals were treated by ozone for 5-10 minutes in a UV chamber, rinsed with excess MQ water and blow dried with air. The QCM chamber and connecting tubes were rinsed with toluene prior to each measurement. Before starting an

experiment, the resistance across the clean and dry crystal in absence of liquid was measured to about 20 Ohm.

Initially the chamber was flushed with pure toluene to obtain a stable baseline. The signal was considered stable when the fluctuation was less than ±5 Hz for half an hour, and this baseline was set to 0 Hz. Next, 10 wt% oil solution (6 ml) was injected by gravitational flow into the measurement chamber, via a temperature loop. The solution was kept in the temperature loop for 300 seconds before exposing it to the crystal surface in the measurement chamber for 10 minutes. The flow conditions remained static while exposing the crystal surface to diluted oil. This procedure was repeated four times in order to ensure saturation of the crystal surface. Finally, toluene was flushed three times over the crystal with relatively high flow rate. The temperature was kept at 25 ± 0.1 ^{o}C. The third overtone of the fundamental resonance frequency was used in the analysis.

Figure 1 shows a representative example of how the frequency (A) and dissipation (B) changed from the baseline upon exposure of the crystal surface (silica) to diluted oil (crude oil-A) followed by flushing with toluene. An immediate drop in resonance frequency was seen when the surface was exposed to the diluted oil, indicating rapid adsorption of the surface-active components. The repeated injections did not alter the frequency significantly, indicating saturation of the crystal surface. Rinsing by toluene resulted in an increase in the frequency before stabilization, which showed that weakly bound components were removed. The corresponding dissipation factor stabilized after rinsing, which confirmed that the remaining components formed a rigid layer at the crystal surface. Then, the irreversibly adsorbed mass was calculated by the Sauerbrey equation. The reproducibility of the experiments was checked by

repeating some of the experiments three time and the calculated masses were differ with the standard error of ~10%.

2.5. Contact Angle Measurements

2.5.1. Air – Water - Mineral Contact Angles

Contact angle measurements were performed on crystals after completing the adsorption measurements using an Optical Contact Angle Meter with a high-speed camera (CAM 200, KSV Instruments). A drop of water (3wt% NaCl in MQ-water) was placed at the coated crystal surface by a Hamilton syringe and images were captured. The contact angles were determined by fitting the Young-Laplace equation to the drop profile. The standard error was less than 5%.

2.5.2. Water – Oil - Mineral Contact Angles

Contact angle measurements of some of the original crude oils (without dilution) were performed directly on the pure crystal surfaces immersed in synthetic seawater. The crystal surfaces were washed following the same procedure as described above. Then the crystals were equilibrated in a cuvette with synthetic seawater at pH 7.8 for 24 hours. The ionic composition of the synthetic sea-water is given in Table 2. An oil drop (not diluted) was placed on the crystal surface when immersed in the aqueous phase. Images were taken by a drop shape analyzer (DSA 100, KRÜSS GmbH Germany). The reported contact angles were determined after 30 minutes, when the drop size did not change significantly. At least four measurements were performed for each system and standard error was less than 5%.

3. RESULTS AND DISCUSSION:

The amounts of adsorbed components at the mineral surfaces and the corresponding alteration of the wettability depended on both the crude oils and the surface composition, Figure 2. The adsorption was generally lowest on the silica surfaces, higher on the aluminosilicate surfaces and highest on the calcium carbonate surfaces, which is in agreement with other reports [29, 41, 42]. The crude oils with the highest asphaltene contents (A, B, D, and E) adsorbed highly at all the surfaces. In addition, crude oil M, which had relatively low asphaltene content but high base content, resulted in high adsorption. Figure 3 shows an increasing trend in adsorbed amounts with both asphaltene content and total base number. This suggested that much of the basic functionalities in the crude oils were present in the asphaltene fractions that adsorbed at the surfaces. The total acid number did not vary systematically with the adsorption or contact angles. Since most of the oils have low acid numbers, any influence of those components on the adsorption would depend more on the molecular structure associated with the acidic groups rather than their quantity. The wax content did not affect the adsorption nor the contact angles, likely due to lack of interfacial activity.

The contact angles prior to adsorption were $18 \pm 2^{\circ}$ for the silica surface, $15 \pm 2^{\circ}$ for the aluminosilicate surface and $55 \pm 5^{\circ}$ for the calcium carbonate surface. In all cases, adsorption reduced the water wettability of the surfaces, Figure 2. For the silica and aluminosilicate surfaces, the contact angles generally increased when the amount of adsorbed components increased. However, some opposite trends were also observed which indicated the selective adsorption of crude oil components on the mineral surfaces e.g. crude oil I was adsorbed low on silica surface compared to aluminosilicate surface but on the contrary contact angle was close to 100 degree on silica surface and only 40 degree on aluminosilicate surface. This showed that smaller but more

hydrophobic fraction was adsorbed on silica and larger but more hydrophilic fraction was adsorbed on aluminosilicate surface. However, more investigations are required to verify this fact. At the calcium carbonate surfaces, the contact angles remained within approximately 60 to 80 degrees, independent of the adsorbed amount. This might indicate a different adsorption mechanism for the latter.

Asphaltenes are polydisperse compounds with an average molecular weight around 750 g/mol, with a factor two in molecular weight distribution [43]. Recent studies indicate that the dominant asphaltene structure consists of 6-7 fused rings constituting an polyaromatic core with alkyl chains attached [44, 45]. The polarity of the asphaltenes is provided by N, O and S present in the structure in form of functional groups such as carbonyls, carboxyls, alcohols, phenols, amines and sulfoxides [14, 46]. The silica surfaces are covered by polar, weakly acidic silanol (Si-OH) groups, which acted as adsorption sites for the polar crude oil components. Hence, the primary adsorption mechanism on silica was polar interactions. Pradilla et al. showed that carboxylic groups were important for the adsorption of model asphaltene compounds at silica, while it was less important for crude oil asphaltenes [42]. Furthermore, Tabrizy et al. demonstrated that a model amine surfactant had high affinity for quartz and kaolinite surfaces [41]. Hence, it can be suggested that amine functionalities at the asphaltenes played an important role in the polar interactions, which is consistent with Figure 3 and similar observations by others [47]. Furthermore, Van der Waals and $\pi - \pi$ interactions were anticipated to contribute. The aluminosilicate surfaces contained *Lewis* acidic aluminol (Al-OH) functional groups in addition to the *Brønsted* acidic silanol groups. This would allow for additional interactions with Lewis basic functional groups, such as amino-nitrogen and sulfoxide-oxygen, in the asphaltenes [48], and can account for the higher amount of adsorbed oil components generally observed at these surfaces. The $CaCO_3$

surface was considerably less hydrophilic than the other surfaces. It has also been shown that carboxylic groups have more prominent contributions to the polar interactions between asphaltenes and $CaCO_3$ surfaces, compared to silica [42]. Furthermore, synergistic effects between asphaltenes and acid surfactants have promoted oil wettability of $CaCO_3$ surfaces [41]. The high adsorption on $CaCO_3$ observed here is probably due to synergies between asphaltenes and acidic components and can thereby be attributed to contributions from both these factors.

The lack of relationship between contact angle and adsorbed amounts for calcium carbonate, opposed to increasing contact angle with increasing adsorption for silica and aluminosilicate surfaces, might imply differences in the orientation of asphaltenes in the two cases. A mix of parallel and perpendicular packing of asphaltenes at surfaces have been suggested [41], while conformational changes of naphthenic acids from parallel to perpendicular orientation have been shown for increasing amounts at silica and calcium carbonate surfaces [29].

Four of the crude oils (A, F, H and L) were exposed to simulated weathering. The physicochemical properties of the weathered fractions are compared with the original values in Table 3. The viscosity and density increased for all the crude oils upon weathering, while the asphaltene fraction either remained the same or increased slightly. Other than for crude oil A, the wax fraction increased in all cases after the simulated weathering. An increase in adsorption, compared to the original crude oils, was also observed in most cases upon the simulated weathering, Figure 4. This was most pronounced at the silica and aluminosilicate surfaces, where the adsorbed mass increased by 36-262% on the silica surfaces and 28-65% on aluminosilicate surfaces. In both cases the increase was largest for the waxy crude oil L and lowest for the asphaltic crude oil A. At the calcium carbonate surfaces, the adsorption increased in the range of

0-28%, highest for the naphthenic crude oil F and lowest for the asphaltic crude oil A. An exception was crude oil A, where the weathering reduced the adsorption. The reason for this is not clear.

It might be speculated that the increased adsorption on the silica and aluminosilicate was related to the increased wax content upon the simulated weathering process. The evaporation of lighter crude oil components changed the solubility conditions and might have promoted adsorption/deposition of parts of the wax fractions. This is supported by the fact that the simulated weathering had minor effects on the contact angles at the surfaces, Figure 5. If the enhanced adsorption were due to asphaltenes, a more marked wettability alteration [18] might have been anticipated.

A dispersant was added to the original and simulated weathered fractions of the four crude oils. Generally, the presence of dispersant reduced the amounts of adsorbed components from both the original oils and weathered fractions, as seen in Figure 4. The reduction was most pronounced for the two oils containing most polar components (i.e. crude oil A and H). This suggested that the dispersant prevented adsorption of some of the crude oil components, either by stabilizing them in the bulk or by occupying adsorption sites at the surfaces and thereby blocking adsorption of oil components. Furthermore, the contact angles were reduced when the dispersant was present, Figure 5. In most cases this reduction corresponded with reduced adsorption on the surfaces.

For comparison between non-aqueous and aqueous environments, contact angle measurements of original crude oils A, F, H and L (without dilution) were performed on the pure mineral surface immersed in synthetic seawater. As shown in Figure 6, the highest contact angles (i.e. most water

wet conditions) were seen at the aluminosilicate surfaces for all the crude oils. The contact angles were slightly lower at the silica surfaces and markedly lower (20-30 degrees; less water wet) at the carbonate surface. This indicated that the interaction of crude oil components was strongest with the calcium carbonate surface, in agreement with the adsorption results. Previous studies have shown that the calcium carbonate surface is positively charged, while the silica and aluminosilicate surfaces are negatively charged at pH 7.8 of the aqueous solution [49]. Furthermore, dissociated acidic components often lower the interfacial tension at these conditions [50], which will provide a negatively charged crude-oil water interface. Consequently, the low contact angles at the calcium surface was attributed to attraction between positively charged carbonate surfaces and negatively charged crude oil-water interface, resulting in the least water wet conditions. Notably, crude oil A, which had highest TAN interacted strongest with the carbonate surface.

4. CONCLUSIONS

The adsorption of crude oil components onto silica, aluminosilicate and calcium carbonate surfaces were studied by the QCM method. The adsorption was attributed to interactions between the polar oil components (asphaltenes as the most important) and hydroxyl groups at the mineral surfaces. The adsorbed amounts varied between the crude oils, but for most oils the adsorption followed the following trend: $CaCO_3 > AlSiO_2 > SiO_2$. Weathering of oils resulted in increased adsorption onto the silica and aluminosilicate surfaces, possibly due to increased wax content, but had no pronounced effect on the calcium carbonate surface. Addition of dispersant reduced the adsorption of both the original crude oils and their weathered fractions. The adsorption was generally accompanied with wettability alterations towards less water wet surfaces, but there were no quantitative relationships between the adsorbed amount and contact angles. In an aqueous environment, the crude oils interacted strongest with calcium carbonate surfaces.

Table 1. Physicochemical Properties of the Crude Oils

Crude oil	TAN (mg KOH/g)	TBN (mg KOH/g)	Aspahltenes (wt%)	Wax (wt%)	Density (g/ml)	Viscosity (mPa·s) at 13°C
A	2.1	3.2	0.9	1.4	0.94	708
B	0.1	2.4	1.2	1.4	0.90	51
C	0.1	1.1	0.5	4.6	0.84	51
D	0.4	7.1	6.6	3.5	0.93	867
E	0.3	1.8	1.8	2.9	0.89	64
F	0.1	-	< 0.1	1.1	0.83	10
G	1.1	1.3	0.1	1.8	0.89	36
H	0.2	1.1	0.4	2.7	0.84	8
I	0.3	2.3	0.6	2.6	0.86	12
J	0.1	-	< 0.1	3.8	0.83	34
K	0.1	1.0	0.2	3.7	0.84	19
L	0.3	-	0.2	4.2	0.88	62
M	0.3	2.0	0.4	4.5	0.85	13

Table 2. Composition of Synthetic Seawater

Salt	g kg−1 solution
Sodium chloride (NaCl)	23.926
Sodium sulfate (Na_2SO_4)	4.008
Potassium chloride (KCl)	0.677
Sodium bicarbonate ($NaHCO_3$)	0.196
Potassium bromide (KBr)	0.098
Boric acid (H_3BO_3)	0.026
Magnesium chloride ($MgCl_2.6H_2O$)	10.831
Calcium chloride ($CaCl_2.2H_20$)	1.5188
Strontium chloride ($SrCl_2.6H_2O$)	0.024

Table 3. Physicochemical Properties of the Crude Oils and 200 °C+ Weathered Fractions

Crude oil		Asphaltenes (wt%)	Wax (wt%)	Viscosity (mPas)	Density (g/mL)
A	Original	0.9	1.4	708	0.94
	200 °C+	1.0	1.4	1085	0.95
F	Original	< 0.1	1.1	10	0.83
	200 °C+	0.1	1.6	85	0.87
H	Original	0.4	2.7	8	0.84
	200 °C+	0.5	3.8	288	0.89
L	Original	0.2	4.2	62	0.88
	200 °C+	0.2	5.7	770	0.89

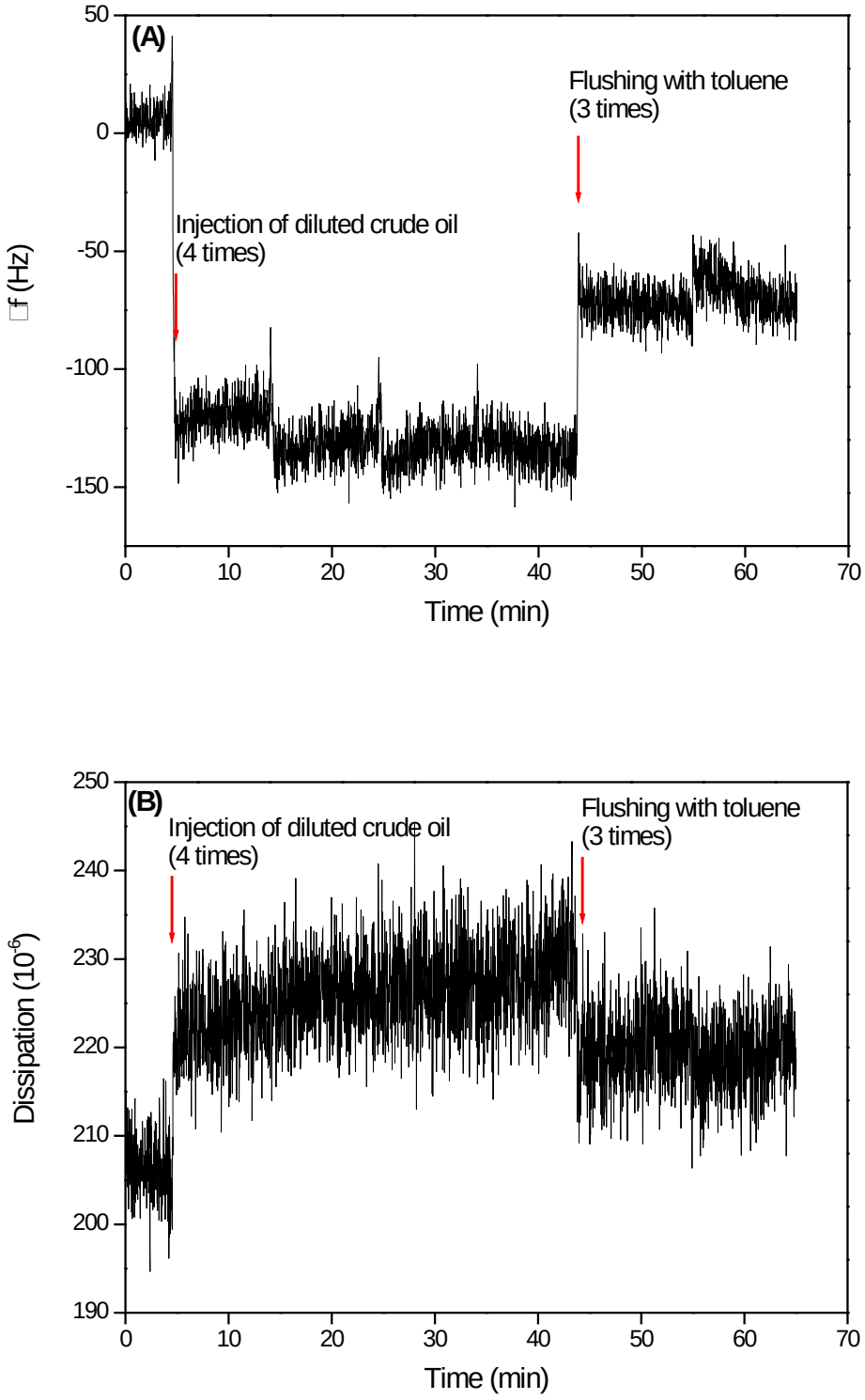

Figure 1. Frequency shift (A) and dissipation shift (B) for a typical measurement sequence with adsorption of crude oil-A components on silica surface followed by flushing with toluene.

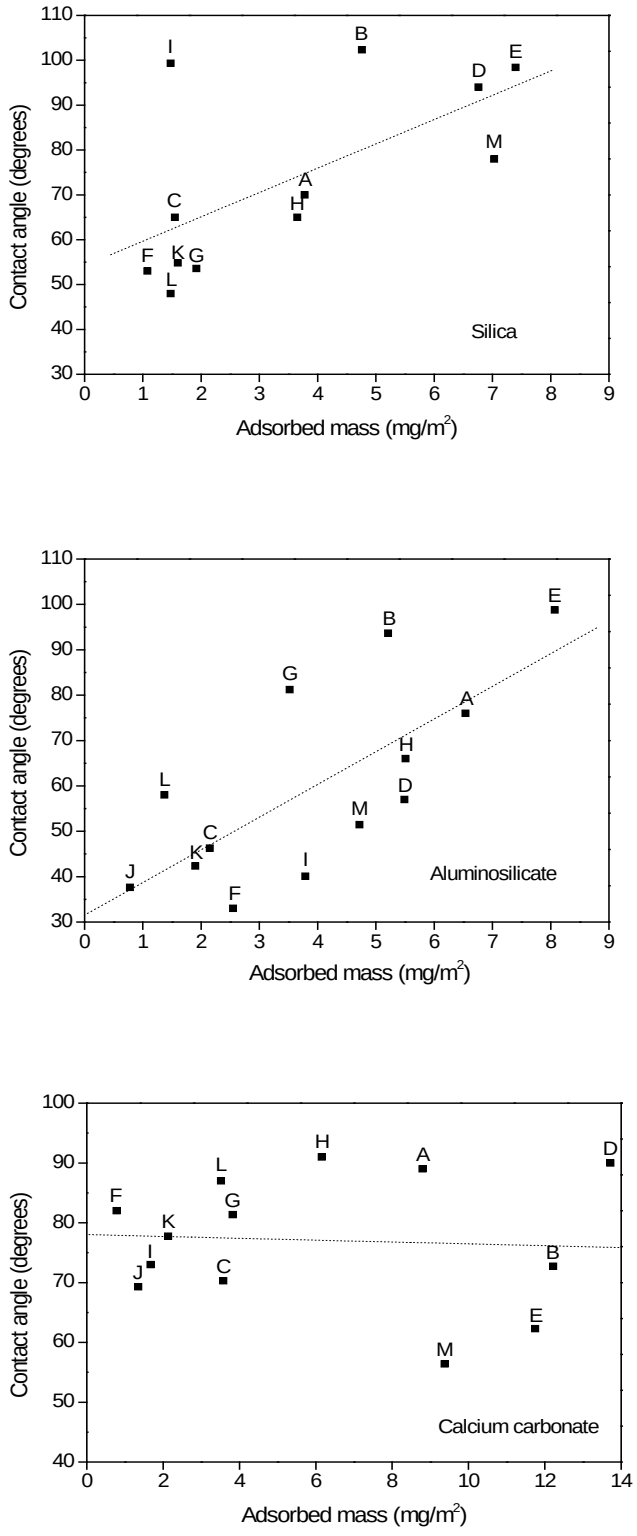

Figure 2. Contact angles plotted against adsorbed mass for silica (top), aluminosilicate (middle) and calcium carbonate (bottom) surfaces. The dotted lines are trend lines.

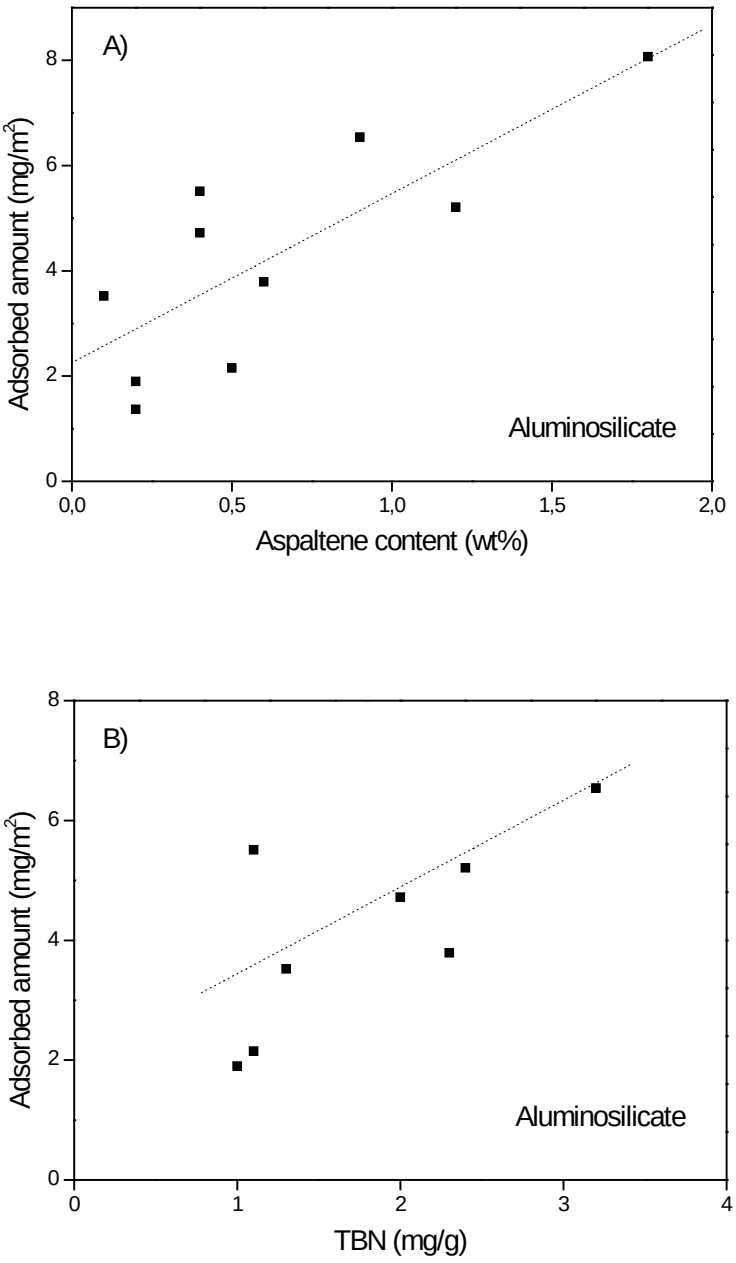

Figure 3. Adsorbed amounts on aluminosilicate surfaces as a function of asphaltene content (A) and TBN (B). For clarity, sample D was not included in the plots. The dotted lines are trend lines.

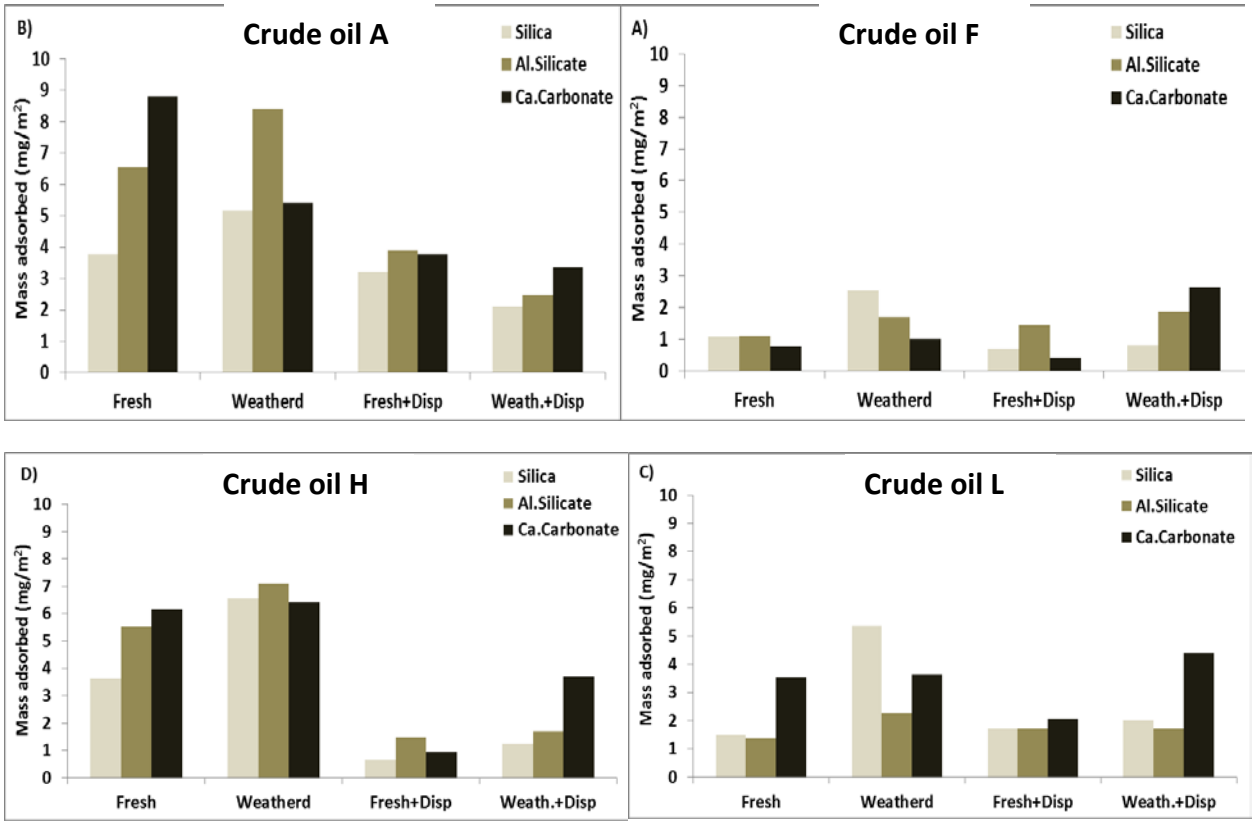

Figure 4. Amount of different oils adsorbed onto different mineral surfaces

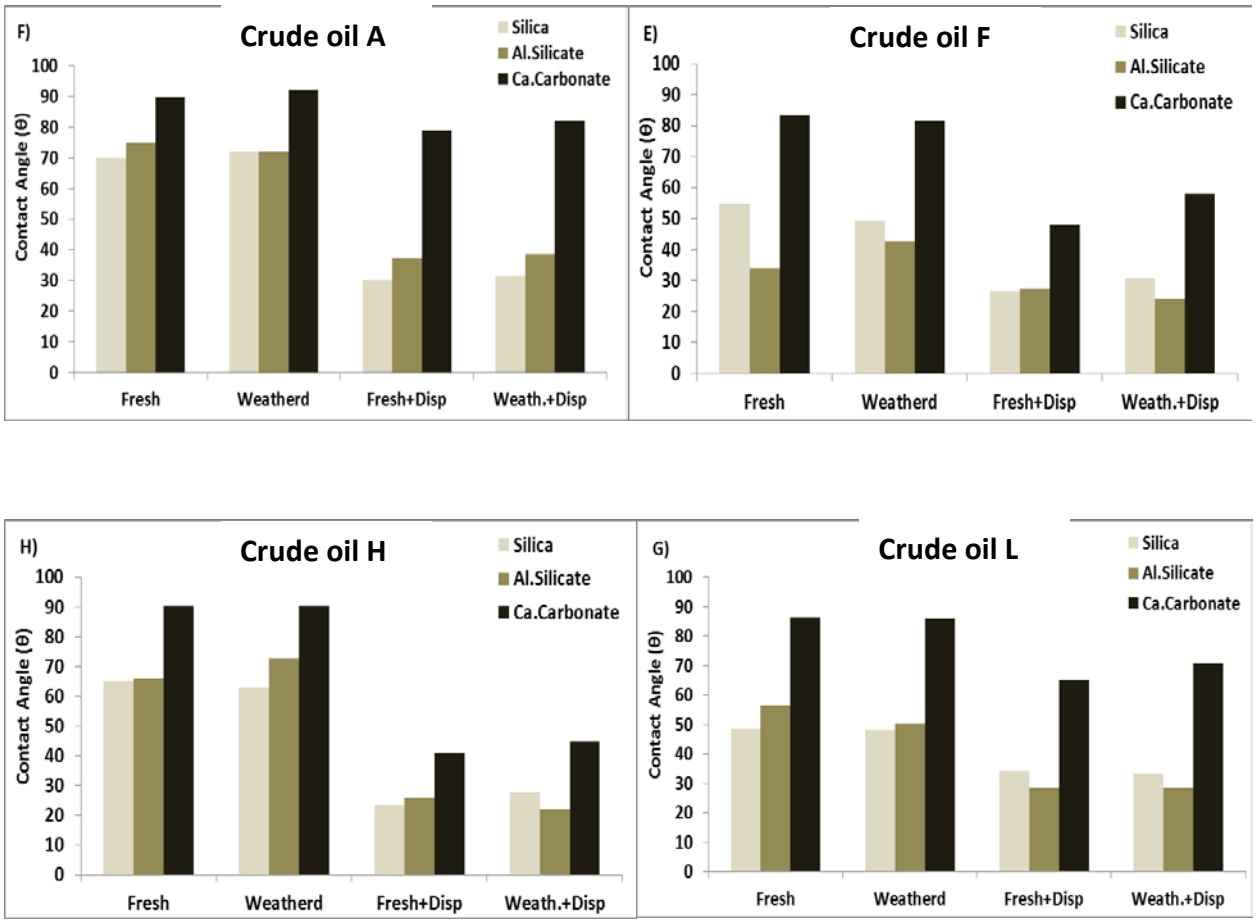

Figure 5. Contact angle of seawater on different surfaces after adsorption of crude oils

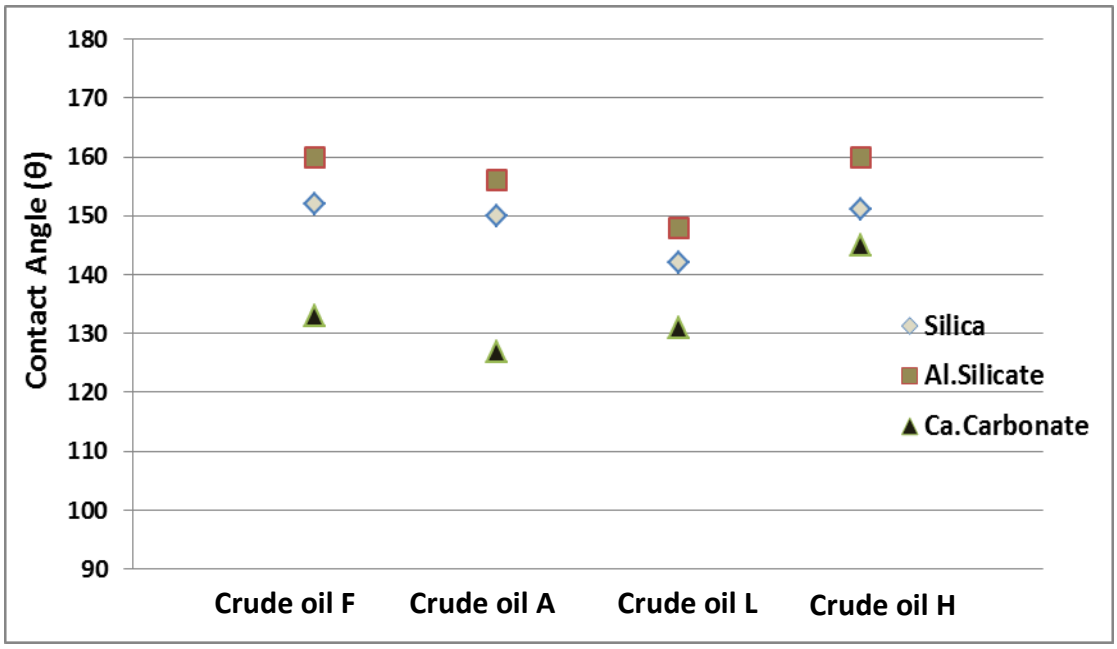

Figure 6. Contact angle of different crude oils on solid surfaces under synthetic seawater

REFERENCES

(1) Anderson, C. M.; LaBelle, R. P. Spill Sci. Technol. Bull. 2000, 6, 303-321..

(2) National Research Council (NRC). Oil in the sea III: Inputs, Fates and Effects. National Academics Press, Washington, DC. 2003.

(3) Camiill, R.; Reddy, C. M.; Yoerger, D. R.; Van Mooy, B. A. S.; Jakuba, M. V.; Kinsey, J. C.; McIntyre, C. P.; Sylva, S. P.; Maloney, J. V. Science, 2010, 330, 201–204..

(4) Graham, W. M.; Condon, R. H.; Carmichael, R. H.; D'Ambra, I.; Patterson, H. K.; Linn, L. J.; Hernandez Jr, F.J . Environ. Res. Lett. 2010, 5, 045301..

(5) Bandara, U. C.; Yapa, P. D.; Xie, H. J. Hydro-environ. Res. 2011, 5, 145–156..

(6) EPA Office of Emergency and Remedial Response, Shoreline Cleanup Of Oil Spills. In Understanding Oil Spills and Oil Spill Responce, pages 17–20. 1999.

(7) Lewis, A.; Daling, P. S.; Kristiansen, T. Strøm.; Nordvik, A. B.; Fiocco, R. J.; Weathering and Chemical Dispersion of Oil at Sea. International Oil Spill Conference Proceedings, American Petroleum Institute, Washington, DC, pp. 157–164. Feb-March 1995.

(8) Fingas, M. The Basics of Oil Spill Cleanup; 3rd Edition, CRC Press, Taylor Francis Group: Boca Raton, 2013; pp 163-188..

(9) Etkin, D. S.; French-McCay, D.; Michel, J. Review of the State-Of-The-Art on Modeling Interactions between Spilled Oil and Shorelines for the Development of Algorithms for Oil Spill Risk Analysis Modeling., MMS U.S Department of the Interior. Environmental Research Consulting, Cortlandt Manor, New York, MMS Contract 0106PO39962. 2007.

(10) Lessard, R. R.; DeMarco, G. Spill Sci. Technol. Bull. 2000, 6, 59–68..

(11) Fiocco, R. J.; Lewis, A. Pure Appl. Chem. 1999, 71, 27–42.

(12) Clayton, J. R.; Payne, J. R.; Farlow, J. S. Oil Spill Dispersants - Mechanisms of Actions and Laboratort Tests. CRC Press, Boca Raton, 1993; pp 14-44.

(13) Klein, G. C.; Angström, A.; Rodgers, R. P.; Marshall, A. G. Energy Fuels. 2006, 20, 668-672..

(14) Gawel, B.; Eftekhardadkhah, M.; Øye, G. Energ Fuels. 2014, 28, 997–1003..

(15) Fingas. M. Introduction to Oil Chemistry and Properties. In Oil Spill Science and Technology, Ed. 1; Elsevier Inc. UK, 2011; pp 51-59..

(16) Kanicky, J. R.; Lopez-Montilla, J-C.; Pandey, S.; Shah, D. O. Surface Chemistry in the Petroleum Industry. In Handbook of Applied Surface and Colloid Chemistry volume 1; John Wiley & Sons, Ltd: New York, 2011; pp 251-270.

(17) Wang, W.; Zheng, Y.; Li, Z.; Lee, K. Chem. Eng. J. 2011, 170, 241-249..

(18) Buckley, J. S.; Liu, Y. J. Pet. Sci. Eng. 1998, 20, 155–160..

(19) Buckley, J. S. Evaluation of reservoir wettability and its effect on oil recovery, First Annual Report, Tulsa, OK, 1997.

(20) Buckley, J. S.; Liu, Y.; Monsterleet, S. SPE J. 1998, 3, 54–61..

(21) Alipour Tabrizy, V. A.; Denoyel, R.; Hamouda, A. A. Colloids Surf., A. 2011, 384, 98–108..

(22) Hadia, N. J.; Hansen, T.; Tweheyo, M. T.; Torsæter, O. Energy Fuels, 2012, 26 (7), 4328−4335.

(23) Hopkins, P. A.; Walrond, K.; Strand, S.; Puntervold, T.; Austad, T.; Wakwaya, A. Energy Fuels. 2016, 30 (9), 7229–7235.

(24) Hutin, A.; Argillier, J-F.; Langevin, D. Oil Gas Sci. Technol.-Rec. IFP Energies nouvelles. 2016, 71, 58.

(25) Farooq, U.; Sjöblom, J.; Øye, G. J. Dispersion Sci. Technol. 2011, 32, 1388-1395.

(26) Farooq, U.; Asif, N.; Tweheyo, M. T.; Sjöblom, J.; Øye, G. Energy Fuels. 2011, 25, 2058-2064.

(27) Ekholm, P.; Blomberg, E.; Claesson, P.; Auflem, I. H.; Sjöblom, J.; Kornfeldt, A. J. Colloid Interface Sci. 2002, 247, 342–350.

(28) Abudu, A.; Goual, L. Energ Fuels. 2009, 23, 1237-1248.

(29) Keleşoğlu, S.; Volden, S.; Kes, M.; Sjöblom, J., Energ Fuels. 2012, 26, 5060-5068..

(30) Grate, J. W.; Dehoff, K. J.; Warner, M. G.; Pittman, J. W.; Wietsma, T. W.; Zhang, C.; Oostrom, M. Langmuir. 2012, 28, 7182−.

(31) Jung, Y. C.; Bhushan, B. Langmuir. 2009, 25 (24), 14165−14173..

(32) Cremaldi, J. C.; Khosla, T.; Jin, K.; Cutting, D.; Wollman, K.; Pesika, N. Langmuir. 2015, 31, 3385−3390.

(33) Broje, V.; Keller. A. A. J. Colloid Interface Sci. 2006, 305, 286-292..

(34) American Society for Testing and Materials (ASTM). ASTM D664, Modified standard test method for Acid number of Petroleum products by Potentiometric Titration; ASTM International: West Conshohocken, PA, 1995..

(35) American Society for Testing and Materials (ASTM). ASTM D2896, Standard test method for base number of Petroleum products by Potentiometric Titration; ASTM International: West Conshohocken, PA, 1995..

(36) Institute of Petroleum (IP). IP 143/90, Asphaltene (Heptane Insolubles) in Petroleum Products, in Standards for Petroleum and its Products, London, UK.

(37) Bridie, A. L.; Wanders, T. H.; Zegweld, W. V.; den Heijde, H. B. Marine Poll. Bull. 1980, 11, 343-348.

(38) American Society for Testing and Materials (ASTM). ASTM D4052-91, Standard Test Method for Density, Relative Density, and API Gravity of Liquids by Digital Density Meter, ASTM International, West Conshohocken, PA, 1991..

(39) McDonagh, M., Hokstad, J. N.; Nordvik, A. B. Standard procedure for viscosity measurement of water-in-oil emulsions. Marine Spill Response Corporation, Washington, DC. MRSC Technical Report Series 95-030. p. 36, 1995.

(40) Mackay, D.; Zagorski, W. Studies of w/o emulsions, Report EE-34: Environment Canada, Ottawa, Ontario, 1982..

(41) Tabrizy, V.A., Denoyel, R., Hamouda, A.A. Coll. Surf. A. 384, 2011, 98-108.

(42) Pradilla, D.; Subramanian, S.; Simon, S.; and Sjöblom, J. Langmuir, 32, 2016, 7294 - 7305.

(43) Groenzin, H. and Mullins, O.C. J. Phys. Chem. A, 103 (50), 1999, 11237–11245.

(44) Sharma, A.; Groenzin, H.; Tomita, A.; and Mullins, O.C. Energy Fuels, 2002, 16 (2), 490–496.

(45) Andrews, A.B.; Edwards, J.C.; Pomerantz, A.E.; Mullins, O.C.; Nordlund, D and Norinaga. K. Energy Fuels, 2011, 25 (7), 3068–3076.

(46) Nourani, M.; Tichelkamp, T.; Gawel, B.; Øye, G. Fuel, 2016, 180, 1-8.

(47) Dudášová, D.; Simon, S.; Hemmingsen, P.V.; Sjöblom, Colloids and Surf. A, 2008, 317, 1-9.

(48) Adams, J. J. Energ Fuels. 2014, 28 (5), 2831–2856.

(49) Farooq, U.; Tweheyo, M.T.; Sjöblom, J.; Øye, G. J. Dispersion Sci. Technol. 2011, 32, 519–531.

(50) Farooq, U.; Simon, S.; Tweheyo, M. T.; Øye, G.; Sjöblom, J. J. Dispersion Sci. Technol. 2013, 34, 701–708.